AAC
Journals.ASM.org

In Vivo Effect of Quaternized Chitosan-Loaded Polymethylmethacrylate Bone Cement on Methicillin-Resistant *Staphylococcus epidermidis* Infection of the Tibial Metaphysis in a Rabbit Model

Hong-lue Tan,[a,b] Hai-yong Ao,[a] Rui Ma,[a] Wen-tao Lin,[a] Ting-ting Tang[a]

Shanghai Key Laboratory of Orthopaedic Implants, Department of Orthopaedic Surgery, Shanghai Ninth People's Hospital, Shanghai Jiao Tong University School of Medicine, Shanghai, China[a]; Luoyang Orthopedics and Traumatology Institute, Luoyang Orthopedic-Traumatological Hospital, Henan, China[b]

Infection of open tibial fractures with contamination remains a challenge for orthopedic surgeons. Local use of antibiotic-impregnated polymethylmethacrylate (PMMA) beads and blocks is a widely used procedure to reduce the risk of infection. However, the development of antibiotic-resistant organisms make the management of infection more difficult. Our *in vitro* study demonstrated that quaternized chitosan (hydroxypropyltrimethyl ammonium chloride chitosan [HACC])-loaded PMMA bone cement exhibits strong antibacterial activity toward antibiotic-resistant bacteria. Therefore, the present study aimed to investigate the *in vivo* antibacterial activity of quaternized chitosan-loaded PMMA. Twenty-four adult female New Zealand White rabbits were used in this study. The right proximal tibial metaphyseal cavity was prepared, 10^7 CFU of methicillin-resistant *Staphylococcus epidermidis* was inoculated, and PMMA-only, gentamicin-loaded PMMA (PMMA-G), chitosan-loaded PMMA (PMMA-C), or HACC-loaded PMMA (PMMA-H) bone cement cylinders were inserted. During the follow-up period, the infections were evaluated using X rays on days 21 and 42 and histopathological and microbiological analyses on day 42 after surgery. Radiographic indications of bone infections, including bone lysis, periosteal reactions, cyst formation, and sequestral bone formation, were evident in the PMMA, PMMA-G, and PMMA-C groups but not in the PMMA-H group. The radiographic scores and gross bone pathological and histopathological scores were significantly lower in the PMMA-H group than in the PMMA, PMMA-G, and PMMA-C groups ($P < 0.05$). Explant cultures also indicated significantly less bacterial growth in the PMMA-H group than in the PMMA, PMMA-G, and PMMA-C groups ($P < 0.01$). We concluded that PMMA-H bone cement can inhibit the development of bone infections in this animal model inoculated with antibiotic-resistant bacteria, thereby demonstrating its potential application for treatment of local infections in open fractures.

Infection of open fractures, which occurs in approximately 24% of open fractures without antibiotic prophylaxis, is a serious complication that can lead to significant morbidity, bone nonunion, and even amputation. Tibiae are more prone to infection than other long bones due to the subcutaneous extent of the shaft, which leads to greater soft tissue stripping and disruption of the vascular supply. In addition, the high-energy injuries that cause tibial fractures also lead to severe contamination of the bone and soft tissue, greatly increasing the risk of infection (1). Infection rates for open tibial fractures are associated with the severity of injury. According to the Gustilo classification, infection rates range from 0 to 2% for type I fractures, from 2% to 10% for type II fractures, and from 10% to 50% for type III fractures (1, 2). Thus, infection related to open tibial fractures remains a challenge for orthopedic surgeons.

To reduce the incidence of infection while managing severe open tibial fractures, local antibiotic-impregnated delivery systems are commonly used as a promising and effective approach to deliver high antibiotic concentrations at the infection site (3, 4). Among the vehicles used clinically for local drug delivery, polymethylmethacrylate (PMMA) bone cements, which are molded into beads or block spacers, remain the standard vehicles for loading antibiotics (4). Aminoglycosides such as gentamicin and tobramycin are the antibiotics most commonly chosen, due to their broad spectra and heat stability (3).

One study of 1,085 open fractures showed an infection rate of 3.7% for fractures treated with antibiotic-impregnated PMMA beads and systemic antibiotic therapy, compared with a 12% infection rate for fractures managed with systemic antibiotic therapy alone (5). Another study showed an obviously lower rate of deep infections in the group treated for open tibial fractures with a bead pouch and delayed primary closure than in the group treated with only delayed wound closure (6). Local antibiotic-impregnated PMMA spacers have also been used successfully in the management of open tibial fractures with large segmental bone loss. Masquelet et al. (7) used a two-stage protocol in which antibiotic-impregnated PMMA cement block spacers were inserted into segmental defects to maintain length and to induce a pseudosynovial membrane, providing a contained space for future cancellous bone grafting.

Antibiotic-impregnated PMMA beads and blocks are useful options for the treatment of severely contaminated open tibial fractures. However, widespread use of antibiotics and prolonged

Received 28 May 2014 Returned for modification 9 July 2014
Accepted 21 July 2014
Published ahead of print 28 July 2014
Address correspondence to Ting-ting Tang, tingtingtang@hotmail.com.

doi:10.1128/AAC.03489-14

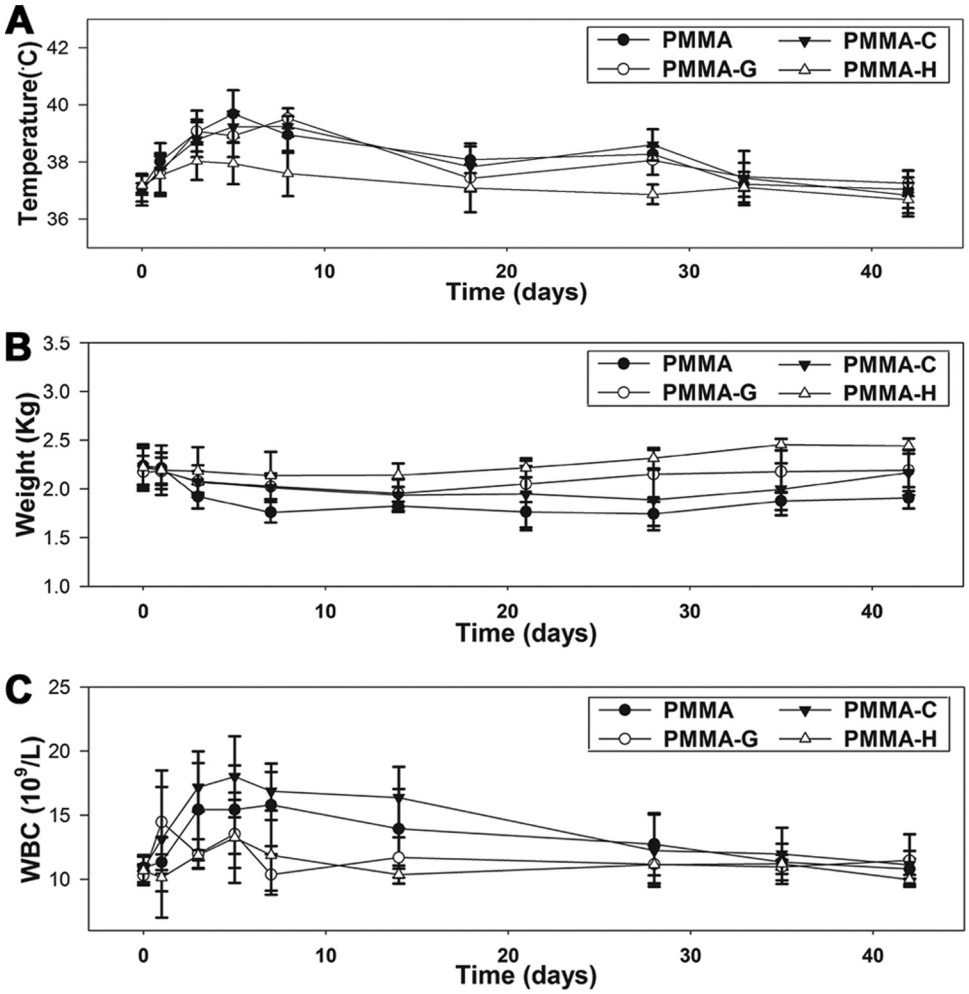

FIG 1 Clinical assessments of animals from various groups. (A) Temperature changes. (B) Weight changes. (C) WBC changes.

implantation with elution of subtherapeutic levels of antibiotic over long periods may lead to the development of antibiotic-resistant organisms (3). *In vitro* studies suggest that up to 8% of the antibiotic in PMMA bone cement is quickly released after surgery, and the low-dose release thereafter may not be effective in fighting infection and may contribute to the problem of antibiotic resistance (8, 9). Gentamicin-resistant *Staphylococcus* and vancomycin-resistant *Staphylococcus aureus* have been increasingly detected (10–12), making the management of infections more difficult. In these cases, the antibiotics in the bone cement have lost their protective effects; therefore, new antimicrobial agents have needed to be investigated constantly in recent years (13).

Chitosan, a naturally biodegradable nontoxic biopolymer, possesses intrinsic activity against a broad spectrum of bacteria, filamentous fungi, and yeasts (14–16). To improve the antibacterial activity and solubility of chitosan, quaternary ammonium chitosan derivatives have been synthesized, and their antibacterial activities have demonstrated significant increases with increasing alkyl substituent chain length (17–21). We synthesized a new quaternized chitosan derivative (hydroxypropyltrimethyl ammonium chloride chitosan [HACC]) that contains a series of quaternary ammonium substitutions, and we found that the antibacterial activities of HACC were enhanced as the quaternary ammonium degree of substitution (DS) increased (18–20). *In vitro* studies demonstrated that HACC-loaded PMMA (PMMA-H) bone cement exhibited strong antibacterial activity and good biocompatibility with osteogenic cells (20, 21). The present study aimed to further investigate the effects of quaternized chitosan-loaded PMMA in infection inhibition in a rabbit model with clinical isolates of methicillin-resistant *Staphylococcus epidermidis* (MRSE) inoculated in the right tibial metaphysis.

MATERIALS AND METHODS

Preparation of bone cements. The bone cements were prepared as in previous studies (20–22). Chitosan or 26% HACC powder (10 g) was added to PMMA polymer powder (40 g) (yielding chitosan-loaded PMMA [PMMA-C] and PMMA-H, respectively), and the components were uniformly mixed at 1,500 rpm for 5 min using a small-scale blender (Speed Mixer model DJ1C; JinTan Technology, Ltd., Jiangsu, China). The cements were prepared by manually combining the powder mixture with the liquid monomer in a bowl until the powder was completely wet. For the *in vivo* study, the mixture was poured into a 4-mm-diameter syringe, and the cements were made into a 1.5-cm-high cylinder with a 4-mm diameter. Plain bone cement (PMMA) and gentamicin-loaded PMMA (PMMA-G) (1 g gentamicin per 40 g PMMA powder) were prepared according to the aforementioned procedure. All cement cylinders were sterilized with 25 kGy of ^{60}Co irradiation prior to use.

Preparation of bacteria. MRSE 287 was isolated from a patient at our hospital (Shanghai Ninth People's Hospital, Shanghai, China) with an orthopedic implant-related infection. MRSE 287 exhibits significant resistance to gentamicin (MIC, 256 μg/ml) and penicillin (MIC, 128 μg/ml). The MIC of HACC with 26% DS against MRSE 287 was previously reported to be 64 μg/ml (20). From an overnight culture of bacteria in 10 ml tryptic soy broth (TSB), 100-μl portions were transferred into sterile tubes containing 10 ml TSB. These tubes were then incubated for 6 h at 37°C to obtain log-phase growth. After incubation, the tubes were centrifuged for 10 min at 3,000 rpm, the supernatant was decanted, and the remaining pellet was washed twice with phosphate-buffered saline (PBS). The bacterial sediment was resuspended in PBS, and the concentration was adjusted to 1×10^8 CFU/ml with TSB, according to the McFarland method. For the *in vivo* studies, a 1-ml bacterial suspension (1×10^8 CFU/ml) was prepared.

Operative procedures. All experiments were approved by the local animal welfare committee. Twenty-four adult female New Zealand White rabbits (2.46 ± 0.23 kg) were used. Surgery was performed under general anesthesia via weight-adapted intramuscular injection of 2% xylazine (12 mg/kg body weight) and ketamine (80 mg/kg body weight). During surgery, the animals were placed in a supine position on sterile drapes, and their bodies were covered with sterile sheets. The right hind limb of each animal was shaved, and the skin was cleaned with Betadine. The tibial tubercle was palpated and identified. An incision over 10 mm in length was made in the skin and fascia at the proximal tibial metaphysis. With a hand-driven titanium burr, a 1-mm hole was drilled through the cortical and cancellous bone to access the medullary cavity at the proximal metaphysis. The medullary cavity was then bluntly reamed with a steel Kirschner wire (4-mm diameter). After removal, 100 μl of Tris-buffered saline (TBS) containing 10^7 CFU MRSE 287 was injected into the medullary cavity. This inoculation dose was selected based on the results of a pilot animal study in which a dose of 10^7 CFU resulted in reliable infection (23). Next, a cylinder of bone cement was inserted, and the skin was carefully sutured layer by layer. No systemic antibiotic treatment was used postsurgery, and the animals were kept in separate cages. The animals were sacrificed after 6 weeks, and their tibiae were harvested under sterile conditions by removing the PMMA bone cement and cutting the tibiae sagittally. The lateral and medial halves were used for microbiological and histological evaluations, respectively. The following groups were investigated in this study: PMMA, PMMA-G, PMMA-C, and PMMA-H. Each group included 6 animals.

Clinical assessment. All animals were monitored on the day of surgery and 1, 3, 5, 7, 14, 28, 35, and 42 days after surgery. The recorded parameters included body weight and temperature, and blood samples were obtained (24–26). The body temperature was measured using a digital infrared thermometer (TERUMO, Zhejiang, China), the weight was determined on a precision scale (TCS, Shanghai, China), and blood samples were obtained from the ear vein to determine white blood cell (WBC) counts. Local clinical signs of infection included swelling and reddening of the right hind limb and loss of passive motion in the knee joint.

Radiographic evaluation. Lateral-view radiographs were obtained on days 21 and 42 after surgery. The radiographic appearances were evaluated according to a modified scoring system (27), as follows: 1, periosteal reaction; 2, osteolysis; 3, soft tissue swelling; 4, deformity; 5, general impression; 6, spontaneous fracture; 7, sequestrum formation. Parameters 1 to 5 were scored as follows: 0, absent; 1, mild; 2, moderate; 3, severe. Parameters 6 and 7 were recorded as 0 (absent) or 1 (present).

Evaluation of gross bone pathology. The animals were sacrificed after 42 days, their tibiae were harvested, and the PMMA bone cement cylinders were removed. Tibiae from each group were then cut sagittally, and the lateral halves were used for gross pathology evaluation (and then the same halves were used for microbiological evaluation). The gross bone pathology scores were determined using the following grading system (28): 0, absence of abscess, sequestra, active bone formation, and erythema; 1, minimal erythema without abscess, sequestra, or evidence of new bone formation; 2, erythema accompanied by widening of the shaft and new bone formation in the bone shaft; 3, abscess with new bone formation, periosteal reaction, sinus tract drainage, or grossly purulent exudate; 4, severe bone resorption, abscess, and diaphyseal or total tibial involvement.

FIG 2 Lateral X-ray photographs of the right tibia, 3 and 6 weeks after surgery. Typical signs include osteolytic lesions (asterisks), periosteal new bone formation (arrowheads), and sequestral bone formation (arrows).

Microbiological evaluation. On the day of sacrifice, the bone cements were explanted, rolled over tryptone soy agar (TSA), and then placed in a 50-ml sterile centrifuge tube containing 10 ml sterile TSB (23–25). The agar plates and TSB were incubated at 37°C for 24 h, after which the CFU on the agar plates were recorded and the bacterial growth in the tryptic soy broth was calculated using serial 10-fold dilutions. From each group, six lateral tibia halves were weighed, chilled with liquid nitrogen, crushed into fragments, and pulverized in a sterile bone mill. The bone powder was homogeneously agitated in 6 ml sterile PBS for 2 min through vortex mixing (Vortex Genie 2; Scientific Industries, Bohemia, NY). The suspension was centrifuged for 10 s at 10,000 rpm, and 100 μl of the supernatant was extracted, serially diluted 10-fold, plated in triplicate on TSA, and incubated at 37°C for 24 h. The CFU on the TSA were counted, and the bacteria level in the bone fragment was determined and expressed relative to the sample weight (CFU/g bone) (24, 25).

Bone histopathology. For histopathology, six medial tibia halves from each group were fixed in 4% buffered formaldehyde for 1 day and decalcified in EDTA for 4 weeks. The decalcified bone samples were embedded in paraffin, and 5-μm longitudinal sections were cut using a microtome

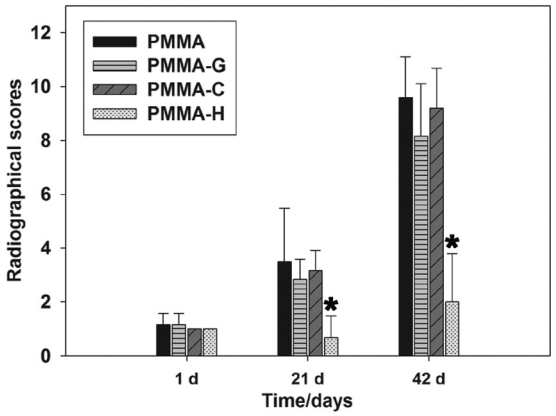

FIG 3 Radiographic scores. Score assessments indicated no significant differences among the PMMA, PMMA-G, and PMMA-C groups ($P > 0.05$). *, $P < 0.05$, compared with the other groups.

(CUT 6062; SLEE Medical, Mainz, Germany). The slides were stained with hematoxylin and eosin for light microscopy. Infections were assessed according to the scoring system described by Smeltzer et al. (29), which included measurements of intraosseous acute inflammation (IAI), intraosseous chronic inflammation (ICI), periosteal inflammation (PI), and bone necrosis (BN).

Statistical analysis. The data were expressed as means ± standard deviations. Differences in body weights, temperatures, WBC counts, and radiographic and histological scores between groups were assessed using one-way analysis of variance (ANOVA) followed by a *post hoc* Tukey's test for multiple comparisons. Nonparametric tests for independent samples (the Mann-Whitney test) were performed for comparison of the gross bone pathology scores and CFU from microbiological evaluations among groups. P values of <0.05 were considered significant. Statistical calculations were performed using SPSS 11.0 software (SPSS, Chicago, IL).

RESULTS

Clinical assessment. Three weeks after surgery, one animal in the PMMA group and one in the PMMA-C group died due to severe infection. The remaining animals recovered well, displaying no evidence of systemic complications during the follow-up period. Six animals in the PMMA and PMMA-C groups and 5 animals in the PMMA-G group presented clear local clinical signs of infection, whereas the animals in the PMMA-H group exhibited no signs of local infection.

The body temperatures of all animals increased gradually from day 1 to day 5. However, the body temperatures of the animals in the PMMA-H group were below those of the animals in the other groups ($P < 0.05$). From day 5 to day 42, the body temperatures of all animals decreased gradually and reached normal levels, with no significant differences between the groups (Fig. 1A). The body weights in the PMMA-H group remained consistent and in-

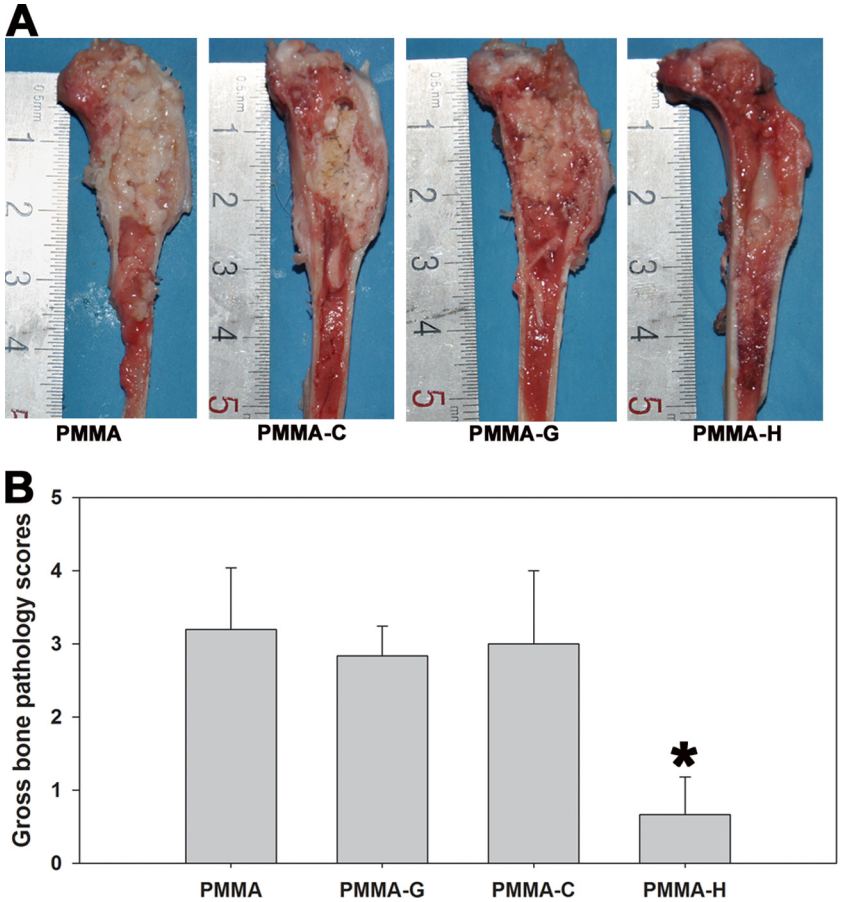

FIG 4 Gross appearance (A) and scores (B) of longitudinal sections of the tibiae. The PMMA, PMMA-G, and PMMA-C groups exhibited signs of purulent infection, while the PMMA-H group presented no obvious signs of infection. *, $P < 0.05$, compared with the other groups.

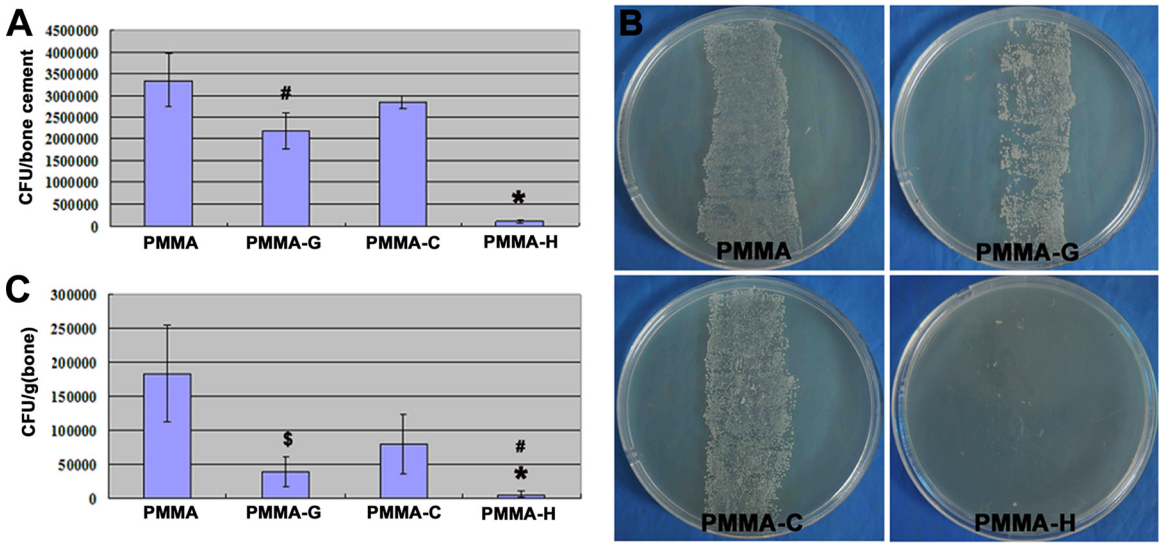

FIG 5 Quantification of bacteria obtained from explanted cements and bone tissue on the day of sacrifice. (A) Quantity of CFU per explanted PMMA-based bone cement. *, $P < 0.01$, compared with other groups; #, $P < 0.05$, compared with the PMMA or PMMA-C group. (B) Growth of bacterial colonies in bone cements on TSA. (C) Quantity of CFU per gram of bone. *, $P < 0.01$, compared with the PMMA or PMMA-C group; #, $P < 0.05$, compared with the PMMA-G group; $, $P < 0.05$, compared with the PMMA or PMMA-C group.

creased slightly during the follow-up period. However, the other three groups exhibited initial decreases in body weight, which increased gradually thereafter. From day 5 to day 42, the body weights in the PMMA group were below those in the PMMA-H group ($P < 0.05$) (Fig. 1B). The WBC counts increased from day 1 to day 5. However, the PMMA-H and PMMA-G groups exhibited lower WBC counts than did the other groups ($P < 0.05$). The WBC counts of all animals decreased gradually from day 5 to day 42 and reached normal levels, with no significant differences between groups, at the time of sacrifice (Fig. 1C).

Radiographic evaluation. Radiographic signs of osteomyelitis were observed in the animals of the PMMA, PMMA-G, and PMMA-C groups. Mild osteolysis was detectable after 3 weeks and became more obvious 6 weeks after surgery, with increases in osteolytic lesions, development of periosteal reactions, new bone formation, and sequestral bone formation (Fig. 2). In animals with PMMA-H bone cement, radiographic signs of infection were nearly absent by day 21, but periosteal reactions were observed at day 42 (Fig. 2).

Quantitative analysis of the X-ray photographs in Fig. 3 determined that the radiographic scores increased gradually after surgery for all four groups. However, the scores indicated no significant differences between the animals in the PMMA, PMMA-G, and PMMA-C groups ($P > 0.05$). The PMMA-H group had significantly lower mean scores than did the other groups ($P < 0.05$). At the time of sacrifice, the mean scores for the PMMA, PMMA-G, PMMA-C, and PMMA-H groups were 9.60 ± 1.52, 8.17 ± 1.94, 9.20 ± 1.48, and 2.00 ± 1.79, respectively.

Gross bone pathology. The PMMA, PMMA-G, and PMMA-C groups demonstrated clear clinical signs of purulent infections, whereas animals in the PMMA-H group appeared free of infection. Particular intramedullary pus formation, osteolytic lesions, periosteal reactions, and bone deformities were the most common clinical symptoms in the infected animals (Fig. 4A). The mean gross bone pathological scores for the PMMA, PMMA-G, PMMA-C, and PMMA-H groups were 3.2 ± 0.84, 2.83 ± 0.41, 3.0 ± 1.0, and 0.67 ± 0.52, respectively (Fig. 4B). No significant differences were noted among the PMMA, PMMA-G, and PMMA-C groups ($P > 0.05$). The mean scores for the PMMA-H group were significantly below those for the other groups ($P < 0.05$).

Microbiological analysis. The cultures obtained from the bone cements of the PMMA-H group had the lowest bacterial loads ($1.0 \times 10^5 \pm 3.4 \times 10^4$ CFU/cement) of the four groups ($P < 0.01$). The mean colony counts for the PMMA-G bone cements ($2.2 \times 10^6 \pm 4.2 \times 10^5$ CFU/cement) after TSB incubation were also significantly lower than those for the PMMA ($3.4 \times 10^6 \pm 6.0 \times 10^5$ CFU/cement) and PMMA-C ($2.8 \times 10^6 \pm 1.5 \times 10^5$ CFU/cement) cements ($P < 0.05$) (Fig. 5A). The rollover cultures from all implants in the PMMA, PMMA-G, and PMMA-C groups revealed massive bacterial growth. In contrast, the implant cultures obtained from the PMMA-H group revealed few bacterial colonies (Fig. 5B).

Figure 5C plots the bacterial load per gram of bone. Significantly lower bacterial loads were achieved in the PMMA-H group ($0.62 \times 10^4 \pm 0.49 \times 10^4$ CFU/g) than in the PMMA ($1.8 \times 10^5 \pm 7 \times 10^4$ CFU/g; $P < 0.01$), PMMA-C ($7.9 \times 10^4 \pm 4.4 \times 10^4$ CFU/g; $P < 0.01$), and PMMA-G ($3.9 \times 10^4 \pm 2.1 \times 10^4$ CFU/g; $P < 0.05$) groups. The PMMA-G group also demonstrated significantly lower bacterial loads than did the PMMA ($P < 0.01$) and PMMA-C ($P < 0.05$) groups.

Histopathological examination. The histopathological sections from the different groups are presented in Fig. 6. Proximal tibial expansion was observed in the PMMA, PMMA-G, and PMMA-C groups, accompanied by bone destruction, bone discontinuity, medullary sequestrum formation, and fibrosis. A large number of acute or chronic inflammatory cells were observed, accompanied by the emergence of tissue necrosis in areas of bone destruction and intramedullary cavities (Fig. 6A to C). However, the proximal tibial tissues of the PMMA-H group exhibited small

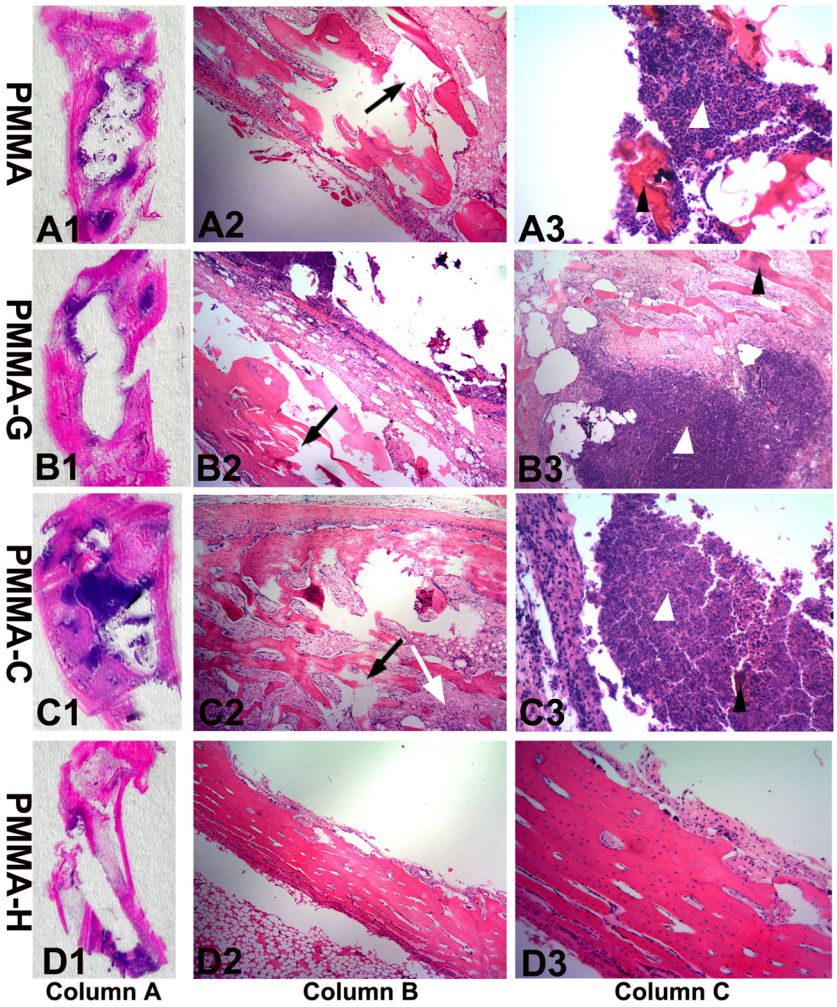

FIG 6 Representative photomicrographs of longitudinal sections from proximal tibiae, with hematoxylin and eosin staining. Column A, overview of signs of osteomyelitis in the proximal metaphysis. Magnification, ×0. Column B, moderate-to-severe inflammation with massive enlargement and destruction of bone tissue (black arrows) and fibrosis (white arrows) in the PMMA, PMMA-G, and PMMA-C groups and mild inflammation in the PMMA-H group. Magnification, ×40. Column C, moderate-to-severe inflammation with intramedullary abscesses and acute or chronic inflammatory cells (white arrowheads) around necrotic bony trabeculae (black arrowheads) in the PMMA, PMMA-G, and PMMA-C groups and mild inflammation in the PMMA-H group. Magnification, ×200.

quantities of inflammatory cell infiltration, bone structure destruction, and necrotic tissue (Fig. 6D). These results suggest that the animals in the PMMA, PMMA-G, and PMMA-C groups showed different degrees of osteomyelitis, including the formation of IAI, ICI, PI, and BN.

The quantitative pathological scores are presented in Fig. 7. In the PMMA and PMMA-C groups, mild-to-moderate or moderate-to-severe IAI accompanied by intramedullary abscesses was observed, resulting in histopathological scores between 3 and 4 (3.6 ± 0.55 and 3.6 ± 0.58 for the PMMA and PMMA-C groups, respectively). ICI with mild-to-moderate or moderate-to-severe chronic inflammation, with or without significant intramedullary fibrosis, was also observed, and the accompanying mean pathological scores for the PMMA and PMMA-C groups were 2.6 ± 0.58 (range, 2 to 3) and 3.3 ± 0.84 (range, 2 to 4), respectively. The mean PI scores (mild-to-moderate or moderate-to-severe chronic inflammation, with or without subperiosteal abscess formation) were 2.4 ± 0.55 (range, 2 to 3) for the PMMA group and 2.8 ± 0.84 (range, 2 to 4) for the PMMA-C group. The BN scores (single

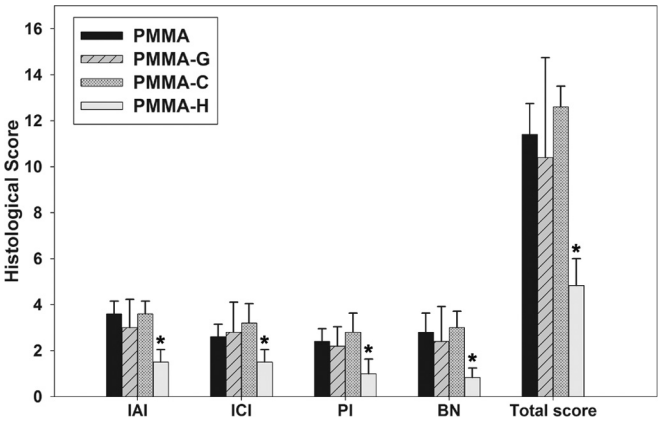

FIG 7 Histological scores for each parameter in each group. The histological intraosseous acute inflammation (IAI), intraosseous chronic inflammation (ICI), periosteal inflammation (PI), and bone necrosis (BN) scores and total scores for the PMMA-H group were significantly lower than those observed in the PMMA, PMMA-G, and PMMA-C groups. *, $P < 0.05$.

or multiple foci of necrosis, with or without sequestrum formation) were 2.8 ± 0.84 and 3.0 ± 0.71 for the PMMA and PMMA-C groups, respectively, and ranged from 2 to 4. In the PMMA-G group, the IAI, ICA, PI, and BN pathological scores were 3.5 ± 0.58 (range, 3 to 4), 3.25 ± 0.96 (range, 2 to 4), 2.5 ± 0.58 (range, 2 to 3), and 3.0 ± 0.82 (range, 2 to 4), respectively.

In the PMMA-H group, the mean IAI score (mild or moderate inflammation without intramedullary abscess formation) was 1.5 ± 0.55 (range, 1 to 2), while the ICI score (mild-to-moderate chronic inflammation with no significant intramedullary fibrosis) was 1.5 ± 0.54 (range, 1 to 2). The PI score (mild-to-moderate chronic inflammation without subperiosteal abscess formation) was 1.0 ± 0.63 (range, 0 to 2), and the BN score (no or single focus of necrosis with no sequestrum formation) was 0.83 ± 0.41 (range, 0 to 1). The mean IAI, ICI, PI, and BN histological scores and the total score are presented in Fig. 7. The mean parameters for the PMMA-H group were significantly lower than those for the PMMA, PMMA-G, and PMMA-G groups ($P < 0.05$).

DISCUSSION

Local use of antibiotic-loaded PMMA bone cement has been the established procedure for treatment of infections of severe open tibial fractures (1, 3). Gentamicin is among the most common antibiotics incorporated into acrylic bone cement, due to its wide antibacterial spectrum and its stability at the high polymerization temperatures required for curing PMMA (8–10, 13, 30). For multidrug-resistant bacteria, however, particularly gentamicin-resistant bacteria, gentamicin-loaded PMMA has proven inadequate for treating or preventing infections. As reported in our previous work, HACC with 26% DS in PMMA bone cements exhibited predictable release kinetics and antibacterial activity for staphylococci (19, 20). In the present study, we further demonstrate the effectiveness of HACC-loaded PMMA in treating bacterial infections in the tibial metaphysis in an animal model.

One well-known cause of postoperative infections of open tibial fractures is severe bacterial pollution at the time of injury. Therefore, we mimicked the operative procedure; MRSE 287 was injected into the prepared proximal tibial metaphyseal cavity of the rabbit and then the PMMA-based bone cement was inserted. Bone infection was verified using X-ray images obtained during the observation period. The validity of this infection model was confirmed because the bone changes were similar to those observed in clinical cases and reported in another study (23).

We compared the effectiveness of PMMA-H in the treatment of infections in the rabbit tibial metaphysis with that of PMMA, PMMA-G, and PMMA-C bone cements by using physical examination, radiographic evaluation, microbiological analysis, and histopathological examination. As evidenced in the *in vivo* experiment, the body temperatures, body weights, and WBC counts of the PMMA-H group did not fluctuate, compared with those of the other groups. Radiographic analysis did not reveal obvious characteristics of bone infections, including bone lysis, cyst formation, and sequestral bone formation, in the PMMA-H group. Significantly lower radiological, gross bone pathological, and histopathological scores were observed in the PMMA-H group, compared with the PMMA, PMMA-G, and PMMA-C groups. These results further demonstrate that PMMA-H bone cement can inhibit the development of bone infections.

The infections caused by MRSE 287 in the PMMA-G and PMMA-C groups were not inhibited, because MRSE 287 is a gentamicin-resistant bacterial strain with an MIC of 256 μg/ml (20). The antibacterial activity of chitosan is also reportedly limited, due to its poor water solubility from PMMA-C cements above pH 6.5 (18). Furthermore, a high-molecular-weight chitosan (molecular weight, 2.0×10^5) was used in the present study, and a previous study conducted in this laboratory demonstrated that this type of chitosan has no antibacterial activity (18). In contrast, infections were obviously inhibited in the PMMA-H group. In agreement with our previous study (20), 26% HACC, which is a quaternary ammonium chitosan, exhibited better water solubility and stronger antibacterial activity than chitosan. Our *in vitro* study demonstrated that 26% HACC-loaded PMMA effectively inhibited bacterial biofilm formation due to its dissolution from the cement surface (20). In the present animal study, the PMMA-H bone cement treated local infections by either inhibiting bacterial adhesion to the bone cement surface or inhibiting the growth of bacteria in the surrounding tissue via HACC dissolution from the cement surface.

In addition, microbiological cultures obtained from the PMMA, PMMA-G, and PMMA-C bone cements exhibited massive growth of MRSA 287 on the implant surface or in the bone tissue. However, although the bacterial colonies formed in the PMMA-H group were significantly smaller than those in the other groups, the bacteria were not completely eradicated, which may be related to the high doses of bacteria (10^7 CFU) inoculated in the metaphyseal cavity of the tibia in this animal model; clinical numbers of contaminating bacteria in the debridement site of the open tibial fractures are much lower. Thus, the local elution of 26% HACC from PMMA-H bone cement may provide protection against bacterial attack and kill the bacteria at the surgical site. In conclusion, the *in vivo* rabbit model with infection in the right tibial metaphysis reported here demonstrated that, compared with PMMA, PMMA-G, and PMMA-C, the HACC-loaded PMMA bone cements significantly inhibited MRSE infections, thereby demonstrating the potential use of PMMA-H as beads, blocks, or temporary spacers for the treatment of local infections in severe open tibial fractures.

ACKNOWLEDGMENTS

This research was financially supported by the National Natural Science Foundation of China (grant 31271015), the NSFC-EU International Cooperation and Exchange Program (grant 51361130034), and the Shanghai Science and Technology Development Fund (grants 13DZ2294000 and 13JC1403900).

REFERENCES

1. **Melvin JS, Dombroski DG, Torbert JT, Kovach SJ, Esterhai JL, Mehta S.** 2010. Open tibial shaft fractures. I. Evaluation and initial wound management. J. Am. Acad. Orthop. Surg. **18:**10–19.
2. **Gustilo RB, Anderson JT.** 1976. Prevention of infection in the treatment of one thousand and twenty-five open fractures of long bones: retrospective and prospective analyses. J. Bone Joint Surg. Am. **58:**453–458.
3. **Zalavras C, Patzakis M, Holtom P.** 2004. Local antibiotic therapy in the treatment of open fractures and osteomyelitis. Clin. Orthop. Relat. Res. **427:**86–93. http://dx.doi.org/10.1097/01.blo.0000143571.18892.8d.
4. **Heffernan EJ, Alkubaidan FO, White LM, Masri BA, Munk PL.** 2007. The radiology of antibiotic-impregnated cement. AJR Am. J. Roentgenol. **189:**446–454. http://dx.doi.org/10.2214/AJR.07.2176.
5. **Ostermann PA, Seligson D, Henry SL.** 1995. Local antibiotic therapy for severe open fractures: a review of 1085 consecutive cases. J. Bone Joint Surg. Br. **77:**93–97.
6. **Keating JF, Blachut PA, O'Brien PJ, Meek RN, Broekhuyse H.** 1996. Reamed nailing of open tibial fractures: does the antibiotic bead pouch

reduce the deep infection rate? J. Orthop. Trauma **10:**298–303. http://dx.doi.org/10.1097/00005131-199607000-00002.
7. **Masquelet AC, Fitoussi F, Begue T, Muller GP.** 2000. Reconstruction of the long bones by the induced membrane and spongy autograft. Ann. Chir. Plast. Esthet. **45:**346–353. (In French.)
8. **Dunne N, Hill J, McAfee P, Todd K, Kirkpatrick R, Tunney M, Patrick S.** 2007. In vitro study of the efficacy of acrylic bone cement loaded with supplementary amounts of gentamicin: effect on mechanical properties, antibiotic release, and biofilm formation. Acta Orthop. **78:**774–785. http://dx.doi.org/10.1080/17453670710014545.
9. **van de Belt H, Neut D, Schenk W, van Horn JR, van der Mei HC, Busscher HJ.** 2000. Gentamicin release from polymethylmethacrylate bone cements and *Staphylococcus aureus* biofilm formation. Acta Orthop. Scand. **71:**625–629. http://dx.doi.org/10.1080/000164700317362280.
10. **Thomes B, Murray P, Bouchier-Hayes D.** 2002. Development of resistant strains of *Staphylococcus epidermidis* on gentamicin-loaded bone cement in vivo. J. Bone Joint Surg. Br. **84:**758–760. http://dx.doi.org/10.1302/0301-620X.84B5.11907.
11. **Anagnostakos K, Hitzler P, Pape D, Kohn D, Kelm J.** 2008. Persistence of bacterial growth on antibiotic-loaded beads: is it actually a problem? Acta Orthop. **79:**302–307. http://dx.doi.org/10.1080/17453670710015120.
12. **Whitener CJ, Park SY, Browne FA, Parent LJ, Julian K, Bozdogan B, Appelbaum PC, Chaitram J, Weigel LM, Jernigan J, McDougal LK, Tenover FC, Fridkin SK.** 2004. Vancomycin-resistant *Staphylococcus aureus* in the absence of vancomycin exposure. Clin. Infect. Dis. **38:**1049–1055. http://dx.doi.org/10.1086/382357.
13. **Tan HL, Lin WT, Tang TT.** 2012. The use of antimicrobial-impregnated PMMA to manage periprosthetic infections: controversial issues and the latest developments. Int. J. Artif. Organs **35:**832–839. http://dx.doi.org/10.5301/ijao.5000163.
14. **Kong M, Chen XG, Xing K, Park HJ.** 2010. Antimicrobial properties of chitosan and mode of action: a state of the art review. Int. J. Food Microbiol. **144:**51–63. http://dx.doi.org/10.1016/j.ijfoodmicro.2010.09.012.
15. **Tayel AA, Moussa S, el-Tras WF, Knittel D, Opwis K, Schollmeyer E.** 2010. Anticandidal action of fungal chitosan against *Candida albicans*. Int. J. Biol. Macromol. **47:**454–457. http://dx.doi.org/10.1016/j.ijbiomac.2010.06.011.
16. **Martinez LR, Mihu MR, Tar M, Cordero RJ, Han G, Friedman AJ, Friedman JM, Nosanchuk JD.** 2010. Demonstration of antibiofilm and antifungal efficacy of chitosan against candidal biofilms, using an in vivo central venous catheter model. J. Infect. Dis. **201:**1436–1440.
17. **Kim CH, Choi JW, Chun HJ, Choi KS.** 1997. Synthesis of chitosan derivatives with quaternary ammonium salt and their antibacterial activity. Polym. Bull. **38:**387–393. http://dx.doi.org/10.1007/s002890050064.
18. **Peng ZX, Wang L, Du L, Guo SR, Wang XQ, Tang TT.** 2010. Adjustment of the antibacterial activity and biocompatibility of hydroxypropyltrimethyl ammonium chloride chitosan by varying the degree of substitution of quaternary ammonium. Carbohydr. Polym. **81:**275–283. http://dx.doi.org/10.1016/j.carbpol.2010.02.008.
19. **Peng ZX, Tu B, Shen Y, Du L, Wang L, Guo SR, Tang TT.** 2011. Quaternized chitosan inhibits *icaA* transcription and biofilm formation by *Staphylococcus* on titanium surface. Antimicrob. Agents Chemother. **55:**860–866. http://dx.doi.org/10.1128/AAC.01005-10.
20. **Tan HL, Peng ZX, Li QT, Xu XF, Guo SR, Tang TT.** 2012. The use of quaternised chitosan-loaded PMMA to inhibit biofilm formation and downregulate the virulence-associated gene expression of antibiotic-resistant staphylococcus. Biomaterials **33:**365–377. http://dx.doi.org/10.1016/j.biomaterials.2011.09.084.
21. **Tan HL, Guo SR, Yang SB, Xu XF, Tang TT.** 2012. Physical characterization and osteogenic activity of the quaternized chitosan-loaded PMMA bone cement. Acta Biomater. **8:**2166–2174. http://dx.doi.org/10.1016/j.actbio.2012.03.013.
22. **Tan HL, Ao HY, Ma R, Tang TT.** 2013. Quaternised chitosan-loaded polymethylmethacrylate bone cement: biomechanical and histological evaluations. J. Orthop. Transl. **1:**57–66. http://dx.doi.org/10.1016/j.jot.2013.06.002.
23. **Alt V, Bitschnau A, Osterling J, Sewing A, Meyer C, Kraus R, Meissner SA, Wenisch S, Domann E, Schnettler R.** 2006. The effects of combined gentamicin-hydroxyapatite coating for cementless joint prostheses on the reduction of infection rates in a rabbit infection prophylaxis model. Biomaterials **27:**4627–4634. http://dx.doi.org/10.1016/j.biomaterials.2006.04.035.
24. **Lucke M, Schmidmaier G, Sadoni S, Wildemann B, Schiller R, Haas NP, Raschke M.** 2003. Gentamicin coating of metallic implants reduces implant-related osteomyelitis in rats. Bone **32:**521–531. http://dx.doi.org/10.1016/S8756-3282(03)00050-4.
25. **Lucke M, Schmidmaier G, Sadoni S, Wildemann B, Schiller R, Stemberger A, Haas NP, Raschke M.** 2003. A new model of implant-related osteomyelitis in rats. J. Biomed. Mater Res. B Appl. Biomater. **67:**593–602. http://dx.doi.org/10.1002/jbm.b.10051.
26. **Jia WT, Luo SH, Zhang CQ, Wang JQ.** 2010. In vitro and in vivo efficacies of teicoplanin-loaded calcium sulfate for treatment of chronic methicillin-resistant *Staphylococcus aureus* osteomyelitis. Antimicrob. Agents Chemother. **54:**170–176. http://dx.doi.org/10.1128/AAC.01122-09.
27. **Rissing JP, Buxton TB, Weinstein RS, Shockley RK.** 1985. Model of experimental chronic osteomyelitis in rats. Infect. Immun. **47:**581–586.
28. **Petty W, Spanier S, Shuster JJ, Silverthrone C.** 1985. The influence of skeletal implants on incidence of infection: experiments in a canine model. J. Bone Joint Surg. Am. **67:**1236–1244.
29. **Smeltzer MS, Thomas JR, Hickmon SG, Skinner RA, Nelson CL, Griffith D, Parr TR, Jr., Evans RP.** 1997. Characterization of rabbit model of staphylococcal osteomyelitis. J. Orthop. Res. **15:**414–421. http://dx.doi.org/10.1002/jor.1100150314.
30. **Virto MR, Frutos P, Torrado S, Frutos G.** 2003. Gentamicin release from modified acrylic bone cements with lactose and hydroxypropylmethylcellulose. Biomaterials **24:**79–87. http://dx.doi.org/10.1016/S0142-9612(02)00254-5.